XANES Study of the Carboxylate Binding Mode in Two Pterin Hydroxylases

by **Ana Mijovilovich**[1])

EMBL-Outstation Hamburg, Notkestrasse 85, Geb 25A, D-22603 Hamburg

Dedicated to Dr. *Celia Saragovi*, celebrating about three decades of work in Applied and Basic Science in Argentina

The 2-His-1-carboxylate triad is an Fe^{II}-binding motif common to several enzyme families. Within the catalytic cycle, the metal ion seems to alter between hexa- and pentacoordination, providing an open space in the Fe moiety for dioxygen binding. Anyhow, based on crystallographic studies, the picture is not fully consistent as different coordination numbers are reported for similar states. Moreover, the orientation of the metal-coordinating carboxylate varies in these studies. These differences are reflected in the XANES spectra analyzed in this paper. For isolated tyrosine and phenylalanine hydroxylase, the different active-site structures postulated by protein crystallography and further improved using spectroscopic data result in calculated XANES pattern that resemble very well the experiments. This work shows that structural differences in the non-coordinated oxygen of the carboxylate have no effect in the EXAFS but cause a change in the white-line intensity that can be successfully modeled within the muffin-tin approximation in small clusters. Thus, the study shows a way to analyze the 'carboxylate shift'. This highlights the potential of XANES analysis and clearly shows that the mentioned structural differences are present in solution as well, and does neither reflect the crystallization artifacts nor result from radiation damage or lacking resolution.

1. Introduction. – The 2-His-1-carboxylate triad is a structural motif shared by a variety of non-heme iron enzyme families that share neither sequence homology nor functionality [1]. Examples are the extradiol-cleaving catechol dioxygenases, the *Rieske* dioxygenases, the isopenicilin N synthase, the deacetoxy-cephalosporin C synthase, and the clavaminate synthase. A further group, the pterin hydroxylases (PAH, TYH, and tryptophan hydroxylase)[2]) require the cofactor tetrahydrobiopterin and a dioxygen molecule for the hydroxylation of an aromatic substrate and the biosynthesis of important neurotransmitters. Dysfunctions in these enzymes cause severe neurological and psychological diseases.

The motif appears associated with processes involving molecular oxygen binding. The metal ion is anchored in the active site by typically three residues spanning the

[1]) Present address: Department of Inorganic Chemistry and Catalysis, University of Utrecht, Sorbonnelaan 16, 3584CA, Utrecht, the Netherlands (phone: +31 30 253 4662; fax: +31 30 251 1027; e-mail: a.e.mijovilovich@uu.nl).

[2]) *Abbreviations:* XAS: X-ray absorption, XANES: X-ray absorption near-edge structure, EXAFS: extended X-ray absorption fine structure, PX: protein crystallography, CD: circular dichroism, MCD: magnetic circular dichroism, PAH: phenylalanine hydroxylase, PaPheOH: *P. aeruginosa* PAH, TYH: tyrosine hydroxylase, *DW: Debye–Waller* parameter.

facial triad: two histidines and one carboxylate group. In *cis*-position, two or three sites are available for binding of oxygen and/or the substrate. This provides flexibility to perform a wide range of catalytic reactions on different substrates that can be oriented by an appropriate protein matrix generally supposed to be determinant of the specificity [1].

Despite these similarities, different coordination numbers and carboxylate-binding modes have been reported for enzymes sharing this motive based on different techniques [2–14] (*Table*). For the pterin-dependent hydroxylases, the crystal structure of TYH [2] at 2.3-Å resolution displays a pentacoordinated metal, while, for PAH [3], an additional H_2O/OH group is identified. In both cases, the coordination number is conserved in the presence of the cofactor biopterin or its analogs [4][9]. By CD/MCD, a change in coordination number from six to five was found for rat phenylalanine hydroxylase, in the presence of a cofactor analogue and the substrate [10].

Table. *EXAFS Distances and* DW *for PaPheOH, and PX Distances for PAH and TYH*

Technique	Sample	First shell distances [Å]: 4 O and 2 N (His)	Second shell distances [Å]: 3 C and OE1-Glu (only for PX)
EXAFS k_{max} 13.5 [1/Å]	PaPheOH Fe^{II} [12]	2.106(6) *DW* [$2x\sigma^2$ 10^{-2}]: 2.30(12)	3.065(22), 3.153(17) (His) 2.952(28) (Glu) *DW* [$2x\sigma^2$ 10^{-2}]: 0.09(49)
EXAFS k_{max} 13.5 [1/Å]	PaPheOH + H_2O_2 Fe^{III} [12]	2.041(3) *DW* [$2x\sigma^2$ 10^{-2}]: 2.77(11)	3.025(24), 3.130(38) (His) 2.980(77) (Glu) *DW* [$2x\sigma^2$ 10^{-2}]: 0.89(98)
PX Res: 2 Å	Human PAH Fe^{III} [3]	2.12 (Glu330), 2.26 (HOH) 2.16 (His290), 2.31 (HOH) 2.17 (His286), 2.34 (HOH)	3.10 (C-Glu330) 3.47 (OE1-Glu330) 3.13, 3.17 (His286) 3.14, 3.15 (His290)
PX Res: 2.3 Å	Rat TYH Fe^{III} [2][9]	2.05 (Glu376), 2.30 (HOH) 2.21 (His331), 2.35 (HOH) 2.35 (His336)	2.64 (C-Glu376) 2.64 (OE1-Glu376) 3.17, 3.19 (His331) 3.29, 3.35 (His336)

Metal coordination can be determined by XAS on liquid samples. In XAS, the edge shape and the pre-edge peak of the Fe K-edge $1s \rightarrow 3d$ transition is sensitive to the Fe-ligand geometry. The intensity of the pre-edge feature increases with the loss of inversion symmetry caused by a decreasing coordination number. This has been studied intensively in model systems [15] and is well-established in the analysis of iron proteins [16][17]. Recently, the richness of the information of the pre-edge peak has been unveiled in Fe catalysts using novel high-resolution K_β detected XANES [18]. Such peak areas for human and *P. aeruginosa* PAH [11][12] confirm hexacoordination. But XAS results comparing the natural [13] with the lyophilized TYH [14] show that natural TYH is hexacoordinated, in disagreement with the crystal structures [2][9]. Potentially, this could have methodological reasons, *e.g.*, differences in pH of the buffer or a lack of resolution of the crystal structure. Moreover, the possibility of photo-reduction during data collection cannot be neglected. Even though the coordination number can be very well determined for Fe sites by analyzing the pre-edge feature,

further details remain unknown. Some unsolved questions are the identity of the missing ligand, the possible modification of the symmetry of the metal site after a change in the coordination numbers, or a change in the distances at the first shell. These questions have mechanistic implications. Changes in the binding mode of carboxylate residues, from monodentate to bidentate, allow keeping a constant coordination number, while providing, at the same time, flexibility for substrate or cofactor binding. Here, XANES simulations are introduced to address the differences between the following three states in solution: *i*) the standard hexacoordinated Fe ion, *ii*) a hexacoordinated Fe ion with an altered carboxylate binding mode, and *iii*) a pentacoordinated Fe ion. These forms are represented by *i*) TYH, *ii*) PAH, and *iii*) PAH pentacoordinated, respectively.

So far, some computer codes have been developed that allow the simulation of XANES for bioinorganic model compounds and metalloproteins. Several attempts for XANES analysis are based on the code CONTINUUM [19]. Its successor, the program MXAN [20], has been tested on superoxide dismutase. The code FDMNES [21] includes full potential calculations by a finite-difference solution of the *Schrödinger*'s equation, instead of the muffin tin potentials used in all other codes. It has been tested also for carbon-monoxy-myoglobin with the purpose of showing the effects of distortions. The FEFF code [22] used here is based on a real-space multiple scattering, which implicitly sums over all final states, without having to calculate them. Full multiple-scattering calculations can be implemented inside a cluster of as much as 100 atoms. It also includes self-consistent field potentials and the core-hole and self-energy effects, the former accounting for the excited state and the latter for the many-body effects and inelastic losses. In a previous paper [23], the predictive capabilities of FEFF applied to BioXANES have been established in these pterin hydroxylases, reproducing the differences in the edge for different oxidation states as well as different coordination numbers. In other recent examples in metalloproteins, FEFF has been successfully used to help determine the number of thiol ligands in Ni-Fe hydrogenases [24] and possible intermediates of the maturation process of the large subunit of this protein [25], and finally, in $Pb^{II}-S$ peptides, FEFF simulations provided evidence that helped determining a tricoordination instead of the known tetracoordination in $Zn^{II}-S_4$ peptides [26].

These parallel efforts by many groups in XANES theory unfortunately have not converged yet in achieving a code including all theoretical features.

The synergy between experiment and simulations in 'BioXANES' is exploited here with emphasis on the carboxylate binding modes in tyrosine hydroxylase compared to phenylalanine hydroxylase. The influence of the orientation of the nonbonded carboxylate O-atom on the XANES pattern is studied. In addition, the sensitivity of these simulations towards changes in the spatial arrangement is evaluated. This allows addition of three-dimensional information to a one-dimensional radial distribution function and will have impact on future XAS studies.

2. Results and Discussion. – Experimental results of the Fe K-edge XANES region of *P. aeruginosa* PAH [12] and human TYH [13] are similar. For the Fe^{II} states, the edge position shifts to lower energies with respect to the Fe^{III} states. Interestingly, the white line for Fe^{II} is slightly higher for TYH than for PAH (*ca.* 8%) for data sets with the same

energy resolution (*ca.* 2.1 eV). Almost no difference is detectable in spectra for Fe^{III} samples of both proteins. XAS Experiments on *P. aeruginosa* PAH [12] and TYH [13] were performed under similar conditions and with identical data-reduction procedures. The lower flux attained with the bending magnet of the former beamline D2 by EMBL (Hamburg; compared to undulator insertion devices) and the low temperatures (*ca.* 30 K) were sufficient for avoiding radiation damage. Thus, the small differences found are not attributable to radiation damage and/or data reduction issues.

The area of the pre-edge feature in the XAS of PaPheOH [12] is identical to the area reported by *Meyer–Klaucke et al.* [13] for isolated human TYH ($6.9 \cdot 10^{-2}$ eV). Thus, the symmetry of the Fe site in both enzymes must be similar.

Overlapping the crystallographic models for the metal sites for human PAH and rat TYH shows that both histidine residues and the iron–carboxylate bond are conserved (*Fig. 1*). Only the unbound O-atom is rotated in TYH with respect to PAH (carboxylate shift). Moreover, two H_2O molecules are reported at similar positions. Only the H_2O in PAH with highest B factor is missing in rat TYH, suggesting high mobility of this metal ligand.

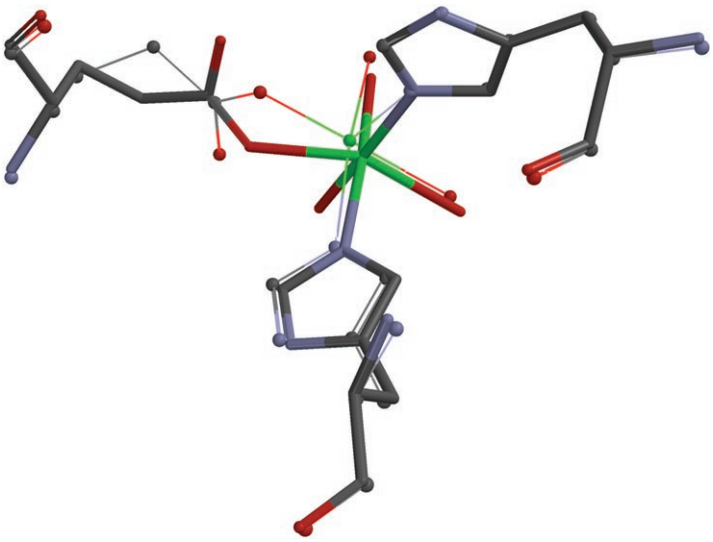

Fig. 1. *Overlapping crystallographic models for TYH* (wire; from 1TOH.pdb) *and PAH* (tube; from 1PAH.pdb) *metal sites, showing the different orientation of the non-coordinating carboxylate O-atom*

In PAH, simulations of the edge reproduced the main features after correcting the coordination shell of the crystallographic data with the distances refined from XAS experiments [23]. In results, the shift towards higher energies of the edge for the higher oxidation state is reproduced.

Though the coordination shell of TYH shown in the crystallographic data is very similar to PAH, the simulations were not able to reproduce the XANES, even when the coordination was completed to six ligands by adding a H_2O, as it is known from XAS that the metal site is hexacoordinated [13].

After turning the carboxylate shown in the TYH crystallographic data with respect to the PAH, the simulation for Fe^{II} reproduces in fact very well the trend in the intensity of the white line for both proteins, with a variation of *ca.* 8% (see *Figs. 2* and *3*). For Fe^{III}, the variation in intensity of the white line is quite small (only 2%).

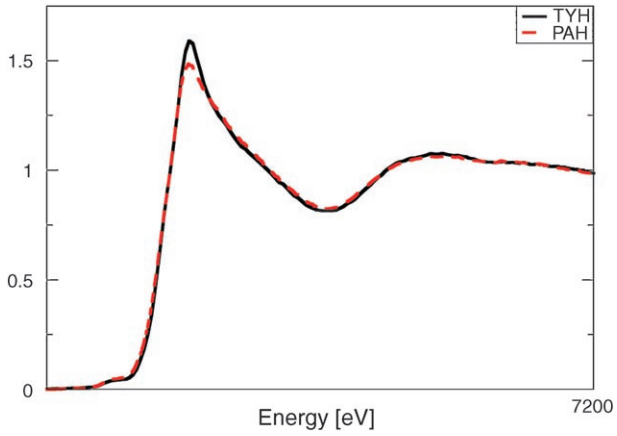

Fig. 2. *Experimental XANES for TYH and PAH* (from [12][13][23])

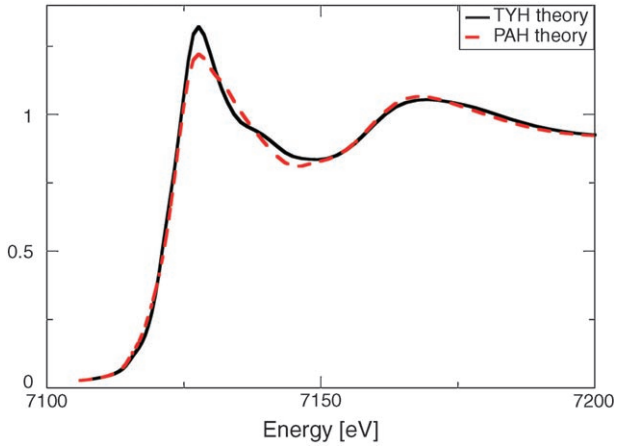

Fig. 3. *XANES Simulations of the Fe-site and the coordinating ligands for TYH and PAH* (last from [23])

The pentacoordinated ferrous PAH was simulated using the same structure after removal of one H_2O (*Fig. 4*). Simulations removing each of the three H_2O molecules (one at a time) were performed, and the results show a reduction in the intensity of the white line ranging from 6 to 10% when compared with the hexacoordinated PAH. This result is qualitatively similar to the tyrosine hydroxylase simulations for penta- and hexacoordination [23]. The lack of the H_2O 426, missing in the crystallographic data for TYH and adjacent to the non-coordinating O-atom OE1 from Glu376, causes the biggest reduction in the intensity of the white line.

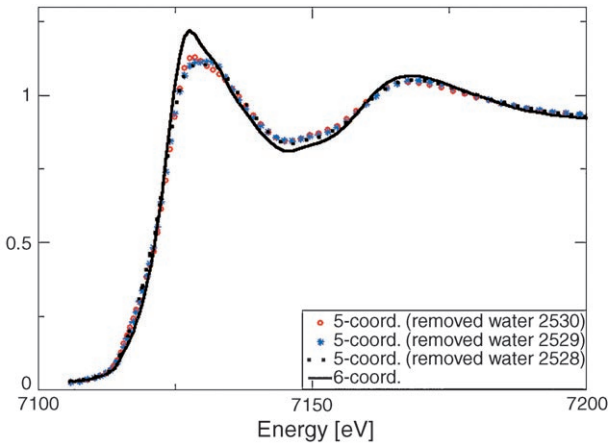

Fig. 4. *XANES Simulation of the Fe-site of PAH for different hydration of the metal: penta- and hexacoordination*

Only the first-coordination-shell amino acids were included, without their backbones. It is known that the mean free path of the photoelectron can be large at the lower energies of the XANES, especially in compounds with lattice periodicity, where the multiple scattering effects have a strong impact on the XANES [22]. In this case, a small cluster was enough to reproduce all the features of the XANES that might be due to the lack of periodic structure around the metal site in proteins.

Also the approximation of the potential by a 'muffin tin' proved to be sufficient in this case. Since the first coordination shell is composed of atoms, which differ in the atomic number by one unit only (N and O), and the symmetry is not highly distorted, this is an ideal case where the 'muffin tin' approximation works well.

The lack of H-atoms in the XANES simulation showed no effect on the overall shape of the XANES. But it is expected to be important for a complete description of the densities of states. Since H-atoms can considerably increase the number of atoms in the calculation, this result has important practical implications for the cluster size of choice.

3. Conclusions. – In both enzymes, any change in the coordination number strongly affects the intensity of the white line and the shape of the second resonance. For the carboxylate rotation, the calculations showed the change of intensity for different orientations of the carboxylate found in the experiment. But in this case, the second resonance remains unaltered for any of the carboxylate orientations, indicating that the effect of the non-coordinated carboxylate O-atom is small in the scattering-dominated region of the spectrum (EXAFS). The second O-atom, more distant to the central absorber, and with a scattering signal that overlaps with the scattering in the imidazole ring, cannot be discerned from EXAFS. Distinguishing carboxylates in a coordination shell including imidazoles is a long standing problem in BioXAS. It is shown in this work that the effect of the carboxylates in the electronic structure, even if small, can be revealed in the XANES region of the XAS spectrum by the XANES simulations. Even

if the 3D structure is not known, careful modeling (eventually including geometrical optimizations) can give more insight on the coordination. This approach has been successfully used to obtain more evidence on the coordination of lead peptides obtained by EXAFS [26].

The change in intensity of the white line might be due to stronger transitions for TYH or a tighter distribution of the transitions contributing to the white line of TYH. In either case, it indicates a change in the electronic structure (increase of bonding and/or effective nuclear charge, or different energies for the molecular orbitals for the two enzymes). Since the XANES is proportional to the density of unoccupied electronic states [27], differences in the white line signal differences in the LUMO and the other first unoccupied levels. More information cannot be extracted from this work, since the H-atoms (which are important for the self-consistent-field calculation of the densities of states, but not for getting the main features of the XANES [22]) were not included.

The simulations were performed using a minimum set of parameters. A key point is the availability of well-defined coordinates as starting model either based on crystallography, EXAFS, or molecular modeling. Given a proper motif, the simulation improves, when adjusting the coordinates to distances refined by EXAFS. Coordination-number changes and differences in the first-shell distances are typical structural questions that can be answered. The perspectives for the method in metalloproteins are very promising in reproducing trends among sets of samples. Furthermore, in this work it is shown that XANES simulations have the capability to show the fine-tuning between the geometrical structure and the features of the XANES spectra. The use of high-resolution XANES, either high-energy resolution fluorescence detected (HERFD) or RIXS detected XANES, will provide more detailed structure of the edge features, as well as the use of excited spectroscopy simulation codes, using a full potential calculation or DFT based codes, will help understanding more complicated metal sites. Studies in this direction are being planned for several proteins of interest in bio-inspired catalysis and their model compounds [28].

Dr. *W. Meyer-Klaucke* (EMBL-Hamburg) is kindly acknowledged for critical reading and useful suggestions in former versions of this manuscript.

Experimental Part

Full details of sample preparation and the XAS experiments and EXAFS analysis will be published elsewhere [12]. a) *Sample Preparation*. The cloning, expression, and purification were performed as reported in [8]. The purity of the protein was analyzed by SDS-PAGE using a *Phastsystem* (*GE*-healthcare). The activity was assayed as described for the recombinant human PAH [29].

b) *XAS Experiments*. Fe K-Edge XAS experiments on PaPheOH were performed at the former D2 EXAFS beamline at the EMBL-Outstation Hamburg as described by *Pohl et al.* [30]. Samples were measured at *ca.* 30 K in a He closed-cycle cryostat in order to avoid radiation damage and to keep the integrity of the proteins. Besides, the low flux of the bending magnet also helped preserving the oxidation state of the samples. The first scans and the last scan (after *ca.* 24 h) were checked for radiation damage. A summary of the refinements using Excurve98 [31] for the samples of this work is shown in the *Table*. The refinements followed the same protocol used in [30].

The protein structures of TYH [2] and PAH [3] were aligned online using DALILITE [32], and the metal sites were plotted using Spartan Student Edition v1.0.2 [33].

FEFF 8.10 [22] has been used to simulate the absorption edges. It includes calculation of self-consistent field potentials and a real-space multiple-scattering theory. The potentials were calculated

with the 'muffin tin' prescription. Neither local symmetry nor periodicity was required, and core-hole and self-energy effects were taken into account. The spectra were calculated using self-consistent 'muffin tin' potentials with 15% overlap. The atomic absorption m_0 was calculated using the ground-state potential with a small constant imaginary part, while, for the excited state, the *Hedin–Lundqvist* exchange correlation potential was used. A cluster size comprising all 19 atoms within a 4.5-Å sphere around the Fe ion and a small charge (1/5 of the valence) allowed reproducing the main features. Increasing the radius up to 5.56 Å and thereby the number of atoms to 30 did not alter the qualitative results. Human PAH, human TYH, and rat TYH share a similar metal center. The simulations of the K-edge XANES spectra of the 2-His 1-carboxylate motif in PAH were based on the crystallographic coordinates for the human protein 1PAH.pdb [3]. Simulations based on the crystal structure 1TOH.pdb for TYH [2] are cumbersome due to the low resolution of the PX data (2.3 Å) and the rather uncertain Fe coordination number in the crystal structures. Thus, simulations for the active site of TYH were based on the more accurately determined coordinates of PAH, with the glutamate shifted to the conformation reported for TYH.

REFERENCES

[1] L. Que Jr., *Nat. Struct. Biol*. **2000**, *7*, 182.
[2] K. E. Goodwill, C. Sabatier, C. Marks, R. Raag, P. F. Fitzpatrick, R. C. Stevens, *Nat. Struct. Biol*. **1997**, *4*, 578.
[3] H. Erlandsen, F. Fusetti, A. Martinez, E. Hough, T. Flatmark, R. C. Stevens, *Nat. Struct. Biol.* **1997**, *4*, 995.
[4] H. Erlandsen, E. Bjørgo, T. Flatmark, R. C. Stevens, *Biochemistry* **2000**, *39*, 2208.
[5] H. Erlandsen, J. Y. Kim, M. G. Patch, A. Han, A. Volner, M. M. Abu-Omar, R. C. Stevens, *J. Mol. Biol.* **2002**, *320*, 645.
[6] B. Kobe, I. G. Jennings, C. M. House, B. J. Michell, K. E. Goodwill, B. D. Santarsiero, R. C. Stevens, R. G. Cotton, B. E. Kemp, *Nat. Struct. Biol.* **1999**, *6*, 442.
[7] O. A. Andersen, T. Flatmark, E. Hough, *J. Mol. Biol.* **2001**, *314*, 279.
[8] F. Ekström, G. Stier, J. T. Eaton, U. H. Sauer, *Acta Crystallogr., Sect. D* **2003**, *59*, 1310.
[9] K. E. Goodwill, C. Sabatier, R. C. Stevens, *Biochemistry* **1998**, *37*, 13437.
[10] J. N. Kemsley, N. Mitic, K. Loeb Zaleski, J. P. Caradonna, E. I. Solomon, *J. Am. Chem. Soc.* **1999**, *121*, 1528.
[11] K. E. Loeb, T. E. Westre, T. J. Kappock, N. Mitić, E. Glasfeld, J. P. Caradonna, B. Hedman, K. O. Hodgson, E. I. Solomon, *J. Am. Chem. Soc.* **1997**, *119*, 1901.
[12] A. Mijovilovich, F. Ekström, W. Meyer-Klaucke, U. Sauer, in preparation.
[13] W. Meyer-Klaucke, H. Winkler, V. Schünemann, A. X. Trautwein, H.-F. Nolting, J. Haavik, *Eur. J. Biochem.* **1996**, *241*, 432.
[14] V. Schünemann, C. Meier, W. Meyer-Klaucke, H. Winkler, A. X. Trautwein, P. M. Knappskog, K. Toska, J. Haavik, *J. Bioinorg. Chem.* **1999**, *4*, 223.
[15] T. E. Westre, P. Kennepohl, J. G. DeWitt, B. Hedman, K. O. Hodgson, E. Solomon, *J. Am. Chem. Soc.* **1997**, *119*, 6297.
[16] A. L. Roe, D. J. Schneider, R. J. Mayer, J. W. Pyrz, J. Widom, L. Que Jr., *J. Am. Chem. Soc.* **1984**, *106*, 1676.
[17] C. R. Randall, Y. Zang, A. E. True, L. Que Jr., *Biochemistry* **1993**, *32*, 6664.
[18] W. M. Heijboer, P. Glatzel, K. R. Sawant, R. F. Lobo, U. Bergmann, R. A. Barrea, D. C. Koningsberger, B. M. Weckhuysen, F. M. F. de Groot, *J. Phys. Chem., B* **2004**, *108*, 10002.
[19] C. R. Natoli, M. Benfatto, *J. Phys. Colloq.* **1986**, *47*, 11.
[20] M. Benfatto, S. Della Longa, *J. Synchrotron Rad.* **2001**, *8*, 1087.
[21] Y. Joly, *Phys. Rev. B* **2001**, *63*, 125120.
[22] A. L. Ankudinov, B. Ravel, J. J. Rehr, S. D. Conradson, *Phys. Rev. B* **1998**, *58*, 7565.
[23] A. Mijovilovich, W. Meyer-Klaucke, *J. Synchrotron Rad.* **2003**, *10*, 64.
[24] T. Burgdorf, S. Löscher, P. Liebisch, E. Van der Linden, M. Galander, F. Lendzian, W. Meyer-Klaucke, S. P. J. Albracht, B. Friedrich, H. Dau, M. Haumann, *J. Am. Chem. Soc.* **2005**, *127*, 576.

[25] S. Löscher, I. Zebger, L. K. Andersen, P. Hildebrandt, W. Meyer-Klaucke, M. Haumann, *FEBS Lett.* **2005**, *579*, 4287.
[26] J. S. Magyar, T.-C. Weng, C. M. Stern, D. F. Dye, B. W. Rous, J. C. Payne, B. M. Bridgewater, A. Mijovilovich, G. Parkin, J. M. Zaleski, J. E. Penner-Hahn, H. A. Godwin, *J. Am. Chem. Soc.* **2005**, *127*, 9495.
[27] F. M. F. De Groot, A. Kotani, 'Core Level Spectroscopies of Solids', Taylor & Francis, New York, 2008.
[28] A. Mijovilovich, H. Hayashi, N. Kawamura, H. Osawa, P. C. A. Bruijnincx, R. J. M. Klein Gebbink, F. M. F. de Groot, B. M. Weckhuysen, International Conference in Bioinorganic Chemistry, ICBIC 13, Vienna, July 15–21, 2007, 'Kβ-detected high-resolution XANES in models of catechol oxygenase'; BIOXAS-Soleil, Gif-sur-Yvette, August 10–11, 2007. August 11th: 'Kβ-detected high-resolution XANES in models of catechol oxygenase'.
[29] A. Martinez, P. M. Knappskog, S. Olafsdottir, A. P. Døskeland, H. G. Eiken, R. M. Svebak, M. Bozzini, J. Apold, T. Flatmark, *Biochem. J.* **1995**, *306*, 589.
[30] E. Pohl, J. C. Haller, A. Mijovilovich, W. Meyer-Klaucke, E. Garman, M. L. Vasil, *Mol. Microbiol.* **2003**, *47*, 903.
[31] N. Binstead, R. W. Strange, S. Hasnain, *Biochemistry* **1992**, *31*, 12117.
[32] DALILITE, Program used here for aligning protein structures: www.ebi.ac.uk.
[33] Spartan, Molecular modeling program, www.wavefun.com.

Received December 31, 2007